Optical gain in rotationally excited nitrogen molecular ions

Ali Azarm, Paul Corkum, and Pavel Polynkin

Phys. Rev. A **96**, 051401 — Published 7 November 2017

DOI: 10.1103/PhysRevA.96.051401

Optical gain in rotationally excited nitrogen molecular ions

Ali Azarm[1], Paul Corkum[2] and Pavel Polynkin[1,*]
[1] *College of Optical Sciences, The University of Arizona, Tucson, Arizona, USA*
[2] *Joint Attosecond Science Laboratory, University of Ottawa and National Research Council, Ottawa, Ontario, Canada KIA 0R6*

We pump low-pressure nitrogen gas with ionizing femtosecond laser pulses at 1.5 μm wavelength. The resulting rotationally excited N_2^+ molecular ions generate directional, forward-propagating stimulated and isotropic spontaneous emissions at 428 nm wavelength. Through high-resolution spectroscopy of these emissions, we quantify rotational population distributions in the upper and lower emission levels. We show that these distributions are shifted with respect to each other, which has a strong influence on the transient optical gain in this system. Although we find that electronic population inversion exists in our particular experiment, we show that sufficient dissimilarity of rotational distributions in the upper and lower emission levels could, in principle, lead to gain without net electronic population inversion.

PACS numbers: 33.80.Eh, 33.20.Sn, 42.55.Lt

Studies of stimulated emission in the constituents of air are motivated by potential applications in air lasing [1], a concept, the realization of which would enable efficient single-ended remote sensing in the atmosphere [2]. Various schemes of turning air into an active laser medium are being investigated [3–6]. One of the most promising approaches is based on pumping atmospheric nitrogen by ultra-intense femtosecond laser pulses propagating in the filamentation regime in air [7]. Intensity inside the core of the femtosecond laser filament is on the order of 100 TW/cm^2, which is sufficient to partially ionize oxygen and nitrogen molecules, producing, in particular, singly-ionized molecular nitrogen ions N_2^+. It has been suggested that air filamentation may result in the optical gain on the electronic transitions of N_2^+ at 391 nm and 428 nm emission wavelengths, as well as on several weaker transitions [8]. However, the gain mechanism responsible for those emissions has been controversial. Apart from its practical potential, air lasing in N_2^+ presents an intriguing problem in intense AMO physics. Indeed, it is counter-intuitive that strong-field ionization of the nitrogen molecule appears to preferentially create a molecular ion in the upper, not the lower emission state. Several alternative gain scenarios have been recently suggested [9–11]. The lack of understanding of the gain mechanism hinders the optimization of the lasing process that could lead to the unseeded lasing in the backward direction, which would be of the most practical significance.

One impediment to progress has been that most experiments involve the interplay of two complex phenomena - filamentation and gain. In the filament, the beam that pumps and probes the gain is irreversibly modified – spectrally, temporally and in its intensity profile. The important parameters for uncovering the physics underlying the gain mechanism are not experimentally accessible.

In this paper, we report the results of a spectroscopic study of spontaneous and stimulated emissions on the transition between the ground vibrational level in the upper electronic energy manifold $B\,^2\Sigma_u^+$ and the first vibrationally excited level in the lower electronic energy manifold $X\,^2\Sigma_g^+$ of N_2^+ (Figure 1, see Supplementary Material for details). These emissions occur at the wavelengths around 428 nm. To disentangle filamentation and gain, we conduct our experiments at low gas pressure and with very tight focusing of the pump beam. Under these conditions, the geometry of the interaction zone is determined by the linear propagation of the focused pump. Although we still probe the gain medium with a co-propagating, spectrally broadened third harmonic of the pump, as we will show below, we are able to estimate the absolute value of optical gain using the well-known spin statistics of nitrogen molecules and the associated degeneracies of different rotational transitions in the N_2^+ molecular ions.

We pump low-pressure nitrogen gas with an intense ultrashort laser pulses at 1,500 nm. The pumping wavelength is chosen to reduce single-photon coupling between the lower emission state $X^2\Sigma_g^+$ and the intermediate state $A^2\Pi_u$ (not shown in Figure 1). In the case of 800 nm pumping, it has been argued that $X^2\Sigma_g^+$ to $A^2\Pi_u$ coupling enables stimulated emission in N_2^+ via population transfer [10, 11]. If $A^2\Pi_u$-state population transfer were key, our use of the 1,500 nm driver would inhibit lasing. Our results show otherwise.

In our experimental setup, 60 fs pulses with an energy of 2 mJ per pulse at 1,500 nm wavelength are generated by an Optical Parametric Amplifier (OPA) pumped by 15 mJ, 60 fs laser pulses at 800 nm. The pulse repetition frequency is 10 Hz. The N_2^+ lasing takes place in a gas cell filled with pure nitrogen gas at a variable pressure. The 15 mm-diameter pump beam is tightly focused inside the gas cell, using a lens with the focal length of 15 cm.

No directional nitrogen lasing is detected in the backward direction (i.e. in the direction opposite to that of the pump beam). In the forward direction, lasing is detected at both 391 nm and 428 nm emission bands of N_2^+, corresponding to the transitions $B^2\Sigma_u^+(0)\rightarrow X^2\Sigma_g^+(0)$ and $B^2\Sigma_u^+(0)\rightarrow X^2\Sigma_g^+(1)$, respectively, where the number in parentheses designates the vibrational level within the

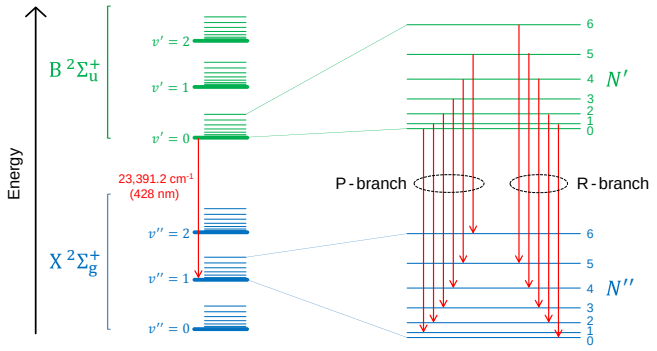

FIG. 1: Left: A diagram of the B $^2\Sigma_u^+$ and X $^2\Sigma_g^+$ electronic energy manifolds of the N_2^+ molecular ion. Integers ν' and ν'' index different vibrational levels within the upper and lower electronic manifolds, respectively. Right: An expanded diagram of vibrational energy manifolds $v' = 0$ and $v'' = 1$ within the upper and lower electronic energy manifolds. N' and N'' are the the nuclear-angular-momentum quantum numbers in the upper and lower emission states, respectively. In the paper, different spectral lines within P and R emission branches are numbered by the quantum number N'' of the lower rotational state involved in the particular transition.

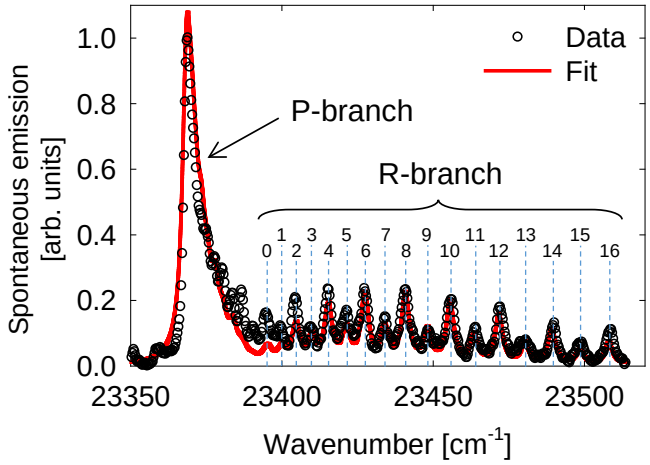

FIG. 2: Experimental data and a fit for spontaneous emission detected from the side, in the case of pumping 4 torr of pure nitrogen with 2 mJ, 60 fs laser pulses at 1,500 nm wavelength. The tabulated values of the wavenumber for different rotational transitions [13] are marked with vertical dashed lines. The corresponding values of the rotational quantum number N'' in the lower emission state are shown next to the individual lines. Spontaneous emission peaks at $N'' = 6$.

electronic state of N_2^+.

The interaction between the 391 nm and 428 nm transitions that share a common upper emission state is beyond the scope of this paper. Here we choose to study the 428 nm emission because of the availability of a Krypton calibration light source with several tabulated spectral lines near the lasing wavelength. The forward-propagating optical signal at 428 nm is directional and linearly polarized in the same way as the pumping beam, indicating that this emission is stimulated and self-seeded by the spectrally broadened third-harmonic of the pump.

Under our experimental conditions, the total energy of the forward-propagating 428 nm emission grows approximately linearly with the gas pressure. For the data shown here, the pressure is set to 4 Torr. Under these conditions, the propagation of the pumping laser beam is unaffected by its nonlinear interaction with the nitrogen in the gas cell. To quantify the parameters of the pump beam in the interaction zone, we have conducted multiple knife-edge measurements of the beam size, inside the low-pressure chamber, at different transverse planes along the propagation path. Thus measured minimum waist radius of the beam at the $1/2e^2$ intensity level is about 60 μm, and the length of the interaction zone is about 1 mm. The peak intensity of the pump beam at the beam waist, inferred from the knife-edge measurements, is about 600 TW/cm^2, which is close to the saturation intensity for the complete single ionization of nitrogen molecules. Using a 1/4 m spectrometer equipped with a 3,600 lines per mm grating, we record spectra of radiation from N_2^+ in the gas cell in the forward direction (self-seeded stimulated emission) and from the side (spontaneous emission). The spectrometer we use has resolution of 9 picometers (0.5 cm^{-1}) in the spectral range of interest around 428 nm wavelength. As we will show below, measuring the spectra of stimulated and spontaneous emissions separately allows us to approximately quantify rotational population distributions of N_2^+ ions in the upper and lower emission levels. The side- and forward-emitted spectra are integrated over 1000 and 100 laser shots, respectively.

The measured spectrum of side emission is shown in Figure 2. The spectrum of spontaneous emission of N_2^+ comprises the so-called P and R branches, which consist of lines with the change of the rotational quantum number N (lower minus upper emission state) of +1 and -1, respectively [12]. The peak value of the P-branch emission is stronger than that of the R-branch, because the P-branch is composed of multiple overlapping emission lines, while the R-branch lines are well separated.

Everywhere in this paper, as well as in the Supplementary Material, we index emission lines in the P and R emission branches by the N'' value of the lower emission state of the corresponding transition. For example, the R-branch emission line indexed with $N'' = 6$ corresponds to the transition from the $N' = 7$ state of the upper electronic energy manifold B $^2\Sigma_u^+(0)$ to the $N'' = 6$ state of the lower electronic energy manifold X $^2\Sigma_g^+(1)$.

The R-branch of the side emission peaks at the N'' value of 6. The placements of the individual spectral lines in the R branch follow their tabulated values [13], shown in Figure 2 with the vertical dashed lines. The amplitudes of the neighboring peaks in the R-branch are different by a factor of 2, which is a consequence of different nuclear-spin multiplicity of states involved in the emissions on the adjacent spectral lines (see the Supplementary Material for details).

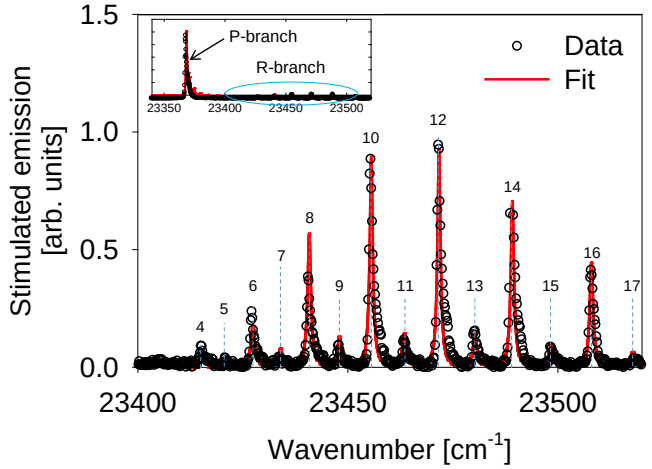

FIG. 3: Same as in Figure 2, but for the stimulated emission that is self-seeded by the spectrally broadened third harmonic of the pump and measured in the forward direction. The R-branch emission, which comprises the transitions with the change of the nuclear angular momentum quantum number N number of -1, is shown in the main figure. The inset shows the full emission spectrum including both P- and R-branch emissions. Stimulated emission peaks at the N'' value of 12, which is larger than the peak value for spontaneous emission. Based on the ratio of the stimulated emission signals on the adjacent spectral lines in the R branch, we estimate the peak value of the total gain, in the 1 mm-long interaction zone as 64, corresponding to the lower-bound estimate for the peak exponential gain per unit length on the strongest R-branch line of about 40 cm^{-1}.

The spectrum of the forward-propagating (stimulated) emission, for the same experimental conditions as those used to measure the spontaneous emission spectrum, is shown in Figure 3. The spectrum of the R-branch emission is shown in the main figure; the complete spectrum including both P and R branches is shown in the inset. In contrast to the case of the spontaneous emission spectrum, the amplitudes of the neighboring emission peaks in the R-branch no longer differ by a factor of two, which is a consequence of the emission process being stimulated.

Due to different nuclear-spin multiplicities of even and odd N-states, the ratio of the values of the exponential gain constants (in the units of cm^{-1}) on the adjacent lines equals 2. Therefore, if the exponential gain constant for the weaker line near the overall peak of the spectral curve is α, the ratio of the amplitudes of the two adjacent stronger and weaker lines equals $e^{2\alpha l}/e^{\alpha l} = G$, where l is the total gain length (which is the same for both the weaker and the stronger lines) and G is the total value of gain on the weaker line. The amplitude ratio for the adjacent spectral peaks, inferred from the measured spectrum, is about 8. Therefore the total value of gain, on the strongest line, can be estimated as 64. The upper estimate of the gain length l is 1 mm, which is the total length of the interaction zone inferred from the knife-edge experiments. Accordingly, the lower-bound estimate of the peak exponential gain per unit length, on the strongest line, is about 40 cm^{-1}. The above estimate is based on the assumption that the overall spectral widths of both the R-branch emission and of the spectrally broadened third harmonic of the pump light, that seeds it, are much larger than the separation between the adjacent spectral lines.

Note that in contrast to the previous studies, e.g., [5] the broad-band pedestal due to the third-harmonic emission that seeds stimulated emission at 428 nm is not visible in the spectrum. That is because our spectrometer has a much higher resolution compared to the spectrometers used in the earlier studies. Generally, if an optical spectrum consists of a broad pedestal and narrow spectral lines that have spectral width much less than the resolution bandwidth of the spectrometer, the detected spectrally broad radiation will be artificially enhanced relative to the narrow spectral lines approximately in proportion to the ratio between the resolution bandwidth and the spectral width of the narrow lines.

Our key experimental observation is that spontaneous emission peaks at the value of the rotational quantum number N'' of about 6, while stimulated emission peaks at a higher value of 12. This experimentally observed difference indicates that the rotational systems in the $\mathrm{B}\,^2\Sigma_u^+(0)$ and $\mathrm{X}\,^2\Sigma_g^+(1)$ states are populated differently. Combined with the $\Delta N = \pm 1$ selection rules, the difference in the rotational population distributions in the two states has a profound effect on the optical gain in this system, as we discuss below. The rotational degree of freedom of N_2^+ is a key physical ingredient of this problem.

We point out that high-resolution measurements of rotational spectra of stimulated emission in N_2^+ under ultrafast laser pumping have been reported previously [14], but not in the connection with the gain mechanism in the N_2^+ ions. The focus of Ref. [14] was on stimulated emission and no spectra of spontaneous emission were reported. Only the difference between stimulated and spontaneous emission spectra is indicative of the rotational effect on the optical gain in N_2^+ that we discuss below.

To fit our experimental data, we parametrize the rotational probability distributions $f'[N']$ and $f''[N'']$, in the upper and lower emission levels $\mathrm{B}\,^2\Sigma_u^+(0)$ and $\mathrm{X}\,^2\Sigma_g^+(1)$, respectively, as follows:

$$f'[N'] \propto \exp\left(-\frac{E'[N'-N_B]}{k_B T_0}\right) \quad (1)$$

$$f''[N''] \propto \exp\left(-\frac{E''[N''-N_X]}{k_B T_0}\right) \quad (2)$$

In the above equations, k_B is the Boltzmann constant and $T_0 = 300\,\mathrm{K}$ is the room temperature. The rotational energies in the upper and lower emission levels are sums of two terms:

$$E'[N'] = B_0 N' \cdot (N'+1) - D_0 \left(N' \cdot (N'+1)\right)^2 , \quad (3)$$

$$E''[N''] = B_1 N'' \cdot (N''+1) - D_1 \left(N'' \cdot (N''+1)\right)^2 \quad (4)$$

where $B_{0,1}$ and $D_{0,1}$ are the N_2^+ ion's rigid and non-rigid rotor constants, respectively, in the upper and lower electronic emission levels. Numerical values for these constants are given in the Supplementary Material [17]. The individual emission peaks are assumed to have the same spectral FWHMs, that are different in the cases of spontaneous and stimulated emission spectra.

Formulas (1),(2) represent Boltzmann-like probability distributions that are coherently shifted in the space of the rotational quantum number by constant values N_B and N_X, which are different for the upper and lower emission states. These shifts are imposed by an impulsive excitation of nitrogen molecular ions by the driver pulse with the duration much shorter than the rotational period of the ions. Shifted Boltzmann distributions in the form (1),(2) have been used previously to describe velocity distributions in ensembles of particles that move, as a whole, with constant speeds (see, for example, [18]).

Needless to say, the ansatz (1),(2) is oversimplified. It is not intended to supplement rigorous analysis that has to account for the interaction of the high intensity laser pulse with the neutral nitrogen molecules [15], the directional dependence of ionization [16] for each electronic state of the ion and the subsequent interaction of the laser field with the ions in $X\,^2\Sigma_g^+$, $A^2\Pi_u$ and $B\,^2\Sigma_u^+$ states. Alternative parametrizations can be used, e.g. Boltzmann distributions with different rotational temperatures in the upper and lower emission levels.

The spectrum of the side (spontaneous) emission is representative of the rotational population distribution in the upper electronic emission level $B\,^2\Sigma_u^+(0)$. It is independent of the rotational distribution in the lower level $X\,^2\Sigma_g^+(1)$. Treating N_B, the overall shift of the Boltzmann rotational distribution (1) in the level $B\,^2\Sigma_u^+(0)$, the FWHM linewidth of the Lorentzian spectral peaks and the overall normalization constant of the spectral curve, as adjustable parameters, we achieve an excellent fit to the experimental data simultaneously for both P and R branches of the spontaneous emission spectrum. The best fit, shown in Figure 2, is obtained with N_B equal to $+2.5$. In the calculation of the fit, we took into account the selection rules for the transitions between different N' and N'' states, as well as the nuclear spin multiplicity and the degeneracy with respect to the projection of the nuclear angular momentum in different rotational energy states. The relative root-mean-square deviation between the experimental data and the fit is 0.016.

After having determined the rotational distribution in the upper emission level $B\,^2\Sigma_u^+(0)$ and the Lorentz FWHM linewidth of the individual spectral peaks $\Delta\nu$, we fit the spectrum of stimulated emission, by varying: (i) the ratio of the total populations in the upper $B\,^2\Sigma_u^+(0)$ and lower $X\,^2\Sigma_g^+(1)$ electronic levels of N_2^+, summed over all rotational states within the two levels, (ii) N_X, the net shift of the rotational distribution (2) in the lower emission level $X\,^2\Sigma_g^+(1)$, (iii) the effective dimensionless gain length l_{eff} and (iv) the overall normalization factor of the spectral curve. The details of the fitting procedures for both spontaneous and stimulated emission spectra are given in the Supplementary Material. We found that the ratio of the total populations in the $B\,^2\Sigma_u^+(0)$ and $X\,^2\Sigma_g^+(1)$ states is predominantly responsible for the relative strengths of the P and R branches in the stimulated emission spectrum, while the shift of the rotational distribution in the lower lasing level, N_X predominantly controls the position of the maximum of the R-branch. The best fit is obtained for the case with net population inversion, with the ratio of populations in the upper and the lower lasing levels equal to 1.35. The best-fit value of the shift of the rotational population in the $X\,^2\Sigma_g^+(1)$ state is $N_X = -1.3$. As in the case of spontaneous emission spectrum, the agreement between the experimentally recorded stimulated emission spectrum and the fit is very good. The relative root-mean-square deviation between the experimental data and the fit is 0.030.

Note that the detected spontaneous emission with the spectrum shown in Figure 2 may have occurred on the time scale longer than the time-scale for the thermalization of the rotational population distribution in the $B\,^2\Sigma_u^+(0)$ state. Consequently, we could have measured an effectively lower value of the distribution shift N_B, in our parametrization (1), than what it was immediately after the impulsive excitation by the ultrashort driver pulse. In order to match the spectrum of stimulated emission shown in Figure 3, we had to correspondingly reduce the value of N_X, the distribution shift in the lower emission state, resulting in the negative value of N_X. Thus parametrized rotational distribution in the $X\,^2\Sigma_g^+(1)$ state turned out to be colder than Boltzmann room-temperature distribution, which may appear to be unphysical.

Although the experimentally measured spectra indicate that an overall electronic population inversion exists between the upper lasing level $B\,^2\Sigma_u^+(0)$ and the lower lasing level $X\,^2\Sigma_g^+(1)$, the net gain involves an additional rotational contribution, which is essential for quantitative description of the experimental data. Figure 4(A) shows the rotational population distributions in the upper and lower emission levels that have been inferred from fitting of the measured spectra. The two allowed transitions that produce strongest spontaneous emission originate from the most populated rotational state in the upper emission level $B\,^2\Sigma_u^+(0)$. These transitions are marked with dashed arrows terminating at the baseline (zero population), indicating that spontaneous emission empties the upper emission state entirely, independently of the population of the lower emission state. The two allowed transitions that produce strongest stimulated emission originate from a different rotational state within the $B\,^2\Sigma_u^+(0)$ level. The solid arrows that mark these transitions terminate not at the baseline but at the populations of the corresponding lower emission states, to indicate that stimulated emission requires population inversion.

In Figure 4(B), we show what would happen if the net

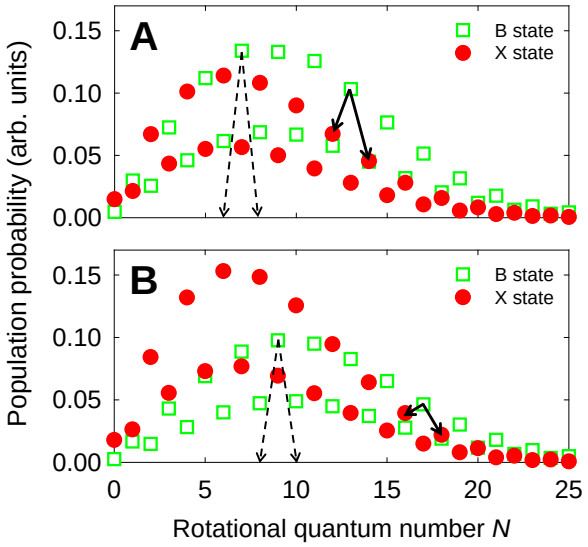

FIG. 4: (A) Rotational population distributions in the upper and lower emission levels of the N_2^+ molecular ion, inferred from fitting of the experimental data. Allowed transitions that produce strongest spontaneous and stimulated emissions are marked with dashed and solid arrows, respectively. (B) Rotational distributions calculated according to (1),(2) with $N_B = 5$ and $N_X = 0$ and negative net electronic population inversion (the ratio of total populations in the $B\,^2\Sigma_u^+(0)$ and $X\,^2\Sigma_g^+(1)$ states equals 0.75). Population inversion and gain still exist on a subset of rotational transitions with large values of the rotational quantum number N.

electronic inversion was negative, but there was a significant shift between rotational distributions in the upper and lower emission levels. Population inversion and gain would still exist on a subset of rotational transitions with high values of rotational quantum number N.

In conclusion, we have reported the results of high-resolution spectroscopic studies of spontaneous and stimulated emissions in singly ionized nitrogen molecules under intense femtosecond pumping at 1,500 nm wavelength. The propagation aspect for the intense pump field was disentangled from the effects involved in the generation of stimulated emission through conducting the experiment at low pressure and using tight focusing for the pump beam. Our results point to a contribution to the gain that is due to a shift between rotational population distributions in the upper and lower emission levels of the N_2^+ molecular ion. The particular mechanism responsible for the generation of dissimilar rotational population distributions in the $B\,^2\Sigma_u^+(0)$ and $X\,^2\Sigma_g^+(1)$ states remains to be found. We show that gain could, in principle, exist even if the net electronic population inversion was negative, provided that rotational population distributions in the upper and lower emission levels were sufficiently dissimilar. Our results suggest the feasibility of the optimization of gain in this system through temporal shaping of the pump pulse.

We thank M. Spanner and M. Ivanov for fruitful discussions. This material is based upon work supported by the US Air Force Office of Scientific Research under MURI award number FA9550-16-1-0013.

* Electronic address: *ppolynkin@optics.arizona.edu*

[1] P. R. Hemmer, R. B. Miles, P. Polynkin, T. Siebert, A. V. Sokolov, P. Sprangle, M. O. Scully, PNAS **108**, 3130 (2011).
[2] P. N. Malevich, R. Maurer, D. Kartashov, S. Ališauskas, A. A. Lanin, A. M. Zheltikov, M. Marangoni, G. Cerullo, A. Baltuška, A. Pugžlys, Opt. Lett. **40**, 2469 (2015).
[3] A. Dogariu, J. Michael, M. Scully, R. Miles, Science **331**, 442 (2011).
[4] A. Laurain, M. Scheller, P. Polynkin, Phys. Rev. Lett. **113**, 253901 (2014).
[5] J. Yao, B. Zeng, H. Xu, G. Li, W. Chu, J. Ni, H. Zhang, S. L. Chin, Y. Cheng, Z. Xu, Phys. Rev. A **84**, 051802(R) (2011).
[6] D. Kartashov, S. Ališauskas, A. Baltuška, A. Schmitt-Sody, W. Roach, P. Polynkin, Phys. Rev. A **88**, 041805(R) (2013).
[7] A. Couairon, A. Mysyrowicz, Phys. Reports **441**, 47 (2007).
[8] Q. Luo, W. Liu, S. L. Chin, Appl. Phys. B **76**, 337 (2003).
[9] Y. Liu, P. Ding, G. Lambert, A. Houard, V. Tikhonchuk, A. Mysyrowicz, Phys. Rev. Lett. **115**, 133203 (2015).
[10] H. Xu, E. Lotstedt, A. Iwasaki, K. Yamanouchi, Nat. Commun. **6**, 8347 (2015).
[11] J. Yao, S. Jiang, W. Chu, B. Zeng, C. Wu, R. Lu, Z. Li, H. Xie, G. Li, C. Yu, Z. Wang, H. Jiang, Q. Gong, Y. Cheng, Phys. Rev. Lett. **116**, 143007 (2016).
[12] G. Herzberg, *Molecular Spectra and Molecular Structure I. Spectra of Diatomic Molecules*, D. Van Nostrand Company, Inc. (1950).
[13] W. H. J. Childs, Proc. Royal Soc. London A **137**, 641 (1932).
[14] H. Xie, B. Zeng, G. Li, W. Chu, H. Zhang, C. Jing, J. Yao, J. Ni, Z. Wang, Z. Li, Y. Cheng, Phys. Rev. A **90**, 042504 (2014).
[15] P. W. Dooley, I. V. Litvinyuk, K. F. Lee, D. M. Rayner, M. Spanner, D. M. Villeneuve, P. B. Corkum, Phys. Rev. A **68**, 023406 (2003).
[16] I. V. Litvinyuk, K. F. Lee, P. W. Dooley, D. M. Rayner, D. M. Villeneuve, P. B. Corkum, Phys. Rev. Lett. **90**, 233003 (2003).
[17] R. R. Laher, F. R. Gilmore, J. Phys. Chem. Ref. Data **20**, 685 (1991).
[18] M. Goossens, *An introduction to plasma astrophysics and magnetohydrodynamics*, Springer Netherlands, Dordrecht, 2003.